

Universe opacity and Type Ia supernova dimming

Václav Vavryčuk,¹★

¹*Institute of Geophysics, The Czech Academy of Sciences, Boční II, Praha 4, 14100, Czech Republic*

Accepted XXX. Received YYY; in original form May 29, 2019

ABSTRACT

In this paper, I revoke a debate about an origin of Type Ia supernova (SN Ia) dimming. I argue that except for a commonly accepted accelerating expansion of the Universe, a conceivable alternative for explaining this observation is universe opacity caused by light extinction by intergalactic dust, even though it is commonly assumed that this effect is negligible. Using data of the Union2.1 SN Ia compilation, I find that the standard Λ CDM model and the opaque universe model fit the SN Ia measurements at redshifts $z < 1.4$ comparably well. The optimum solution for the opaque universe model is characterized by the B-band intergalactic opacity $\lambda_B = 0.10 \pm 0.03 \text{ Gpc}^{-1}$ and the Hubble constant $H_0 = 68.0 \pm 2.5 \text{ km s}^{-1} \text{ Mpc}^{-1}$. The intergalactic opacity is higher than that obtained from independent observations but still within acceptable limits. This result emphasizes that the issue of the accelerating expansion of the Universe as the origin of the SN Ia dimming is not yet definitely resolved. Obviously, the opaque universe model as an alternative to the Λ CDM model is attractive, because it avoids puzzles and controversies associated with dark energy and the accelerating expansion.

Key words: dust, extinction – opacity – dark energy – supernovae – intergalactic medium

1 INTRODUCTION

Type Ia supernovae (SNe Ia) dimming is one of the most exciting discoveries in astronomy in the last 20 years. The first results published by [Riess et al. \(1998\)](#) and [Perlmutter et al. \(1999\)](#) were based on measurements of 16 and 42 high-redshift SNe Ia, respectively. However, observations of the unexpected SNe Ia dimming motivated large-scale systematic searches for SNe Ia and resulted in a rapid extension of supernovae compilations ([Sullivan et al. 2011](#); [Suzuki et al. 2012](#); [Campbell et al. 2013](#); [Betoule et al. 2014](#); [Jones et al. 2018](#); [Scolnic et al. 2018](#)). This surprising phenomenon was explained by an accelerating expansion of the Universe, and consequently a concept of the cosmological constant ([Einstein 1917](#); [Blome & Priester 1985](#); [Carroll et al. 1992](#)) was revived and reintroduced as dark energy into the cosmological models ([Weinberg 1989](#); [Riess 2000](#); [Sahni & Starobinsky 2000](#); [Peebles & Ratra 2003](#)).

Processing of the SNe Ia data is not straightforward. Prior to interpretations, corrections must be applied to transform an observed-frame magnitude to a rest-frame magnitude. This includes a cross-filter K -correction and a correction for light extinction due to absorption by dust in the host galaxy and in our Galaxy ([Perlmutter et al. 1999](#); [Nugent et al. 2002](#); [Riess et al. 2004](#)). The uncertain-

ties in the extinction corrections are in general much higher than those in the K -corrections ([Nugent et al. 2002](#)). Moreover, the uncertainties increase due to neglecting redshift-dependent extinction by intergalactic dust which might display different reddening than the interstellar dust ([Ménard et al. 2010b](#)). Obviously, these uncertainties raise the question, whether the observations of supernovae dimming are not partly or fully a product of intergalactic extinction.

Intergalactic opacity as a possible origin of dimming of the SNe Ia luminosity was proposed by [Aguirre \(1999a,b\)](#) and [Aguirre & Haiman \(2000\)](#). Also [Ménard et al. \(2010b\)](#) point out that a reddening-based correction is not sensitive to intergalactic opacity and it might bias the calculated distance modulus and the cosmological parameters describing the accelerating expansion. This problem was also addressed by [Riess et al. \(2004\)](#) who found that some models of intergalactic dust might produce a similar dimming as observed and interpreted by the accelerating expansion. The authors fitted a theoretical extinction curve to the SNe Ia dimming in the redshift interval $z < 0.5$. They found a satisfactory fit, but a remarkable discrepancy appeared at higher z , see [Goobar et al. \(2002, their fig. 3, model A\)](#) or [Riess et al. \(2004, their fig. 7, 'high- \$z\$ gray dust' model\)](#). The discrepancy was removed for a redshift-independent proper density of intergalactic dust for $z > 0.5$, however, this contradicts the idea of an increasing proper density of intergalactic dust due to the smaller volume of the Universe in the past.

★ E-mail: vv@ig.cas.cz

In this paper, I revisit this analysis and argue that rejecting the universe opacity as a possible origin of SNe Ia dimming was not fully justified. I show that intergalactic dust might produce similar effects in the SNe Ia dimming as the accelerating expansion. The proposed opacity model is characterized by an increase of the proper dust density with redshift for all z but not only for $z < 0.5$ as suggested by [Goobar et al. \(2002\)](#) and [Riess et al. \(2004\)](#). The model fits the SNe Ia data comparably well as the currently used Λ CDM model does. Advantageously, the proposed model does not need the controversial dark energy concept and the accelerating expansion.

2 INTERGALACTIC OPACITY

The intergalactic opacity λ_V (defined as attenuation A_V of intergalactic space per unit ray path) is caused by light extinction by intergalactic dust and it is spatially and redshift dependent. It is mostly appreciable at close distance from galaxies and in intracluster space. [Ménard et al. \(2010a\)](#) report visual intergalactic attenuation $A_V = (1.3 \pm 0.1) \times 10^{-2}$ mag at distance from a galaxy of up to 170 kpc and $A_V = (1.3 \pm 0.3) \times 10^{-3}$ mag at distance of up to 1.7 Mpc. Similar values are observed for the visual attenuation of intracluster dust ([Muller et al. 2008](#); [Chelouche et al. 2007](#)). An averaged value of intergalactic extinction was measured by [Ménard et al. \(2010a\)](#) by correlating the brightness of $\approx 85,000$ quasars at $z > 1$ with the position of 24 million galaxies at $z \approx 0.3$ derived from the Sloan Digital Sky Survey. The authors estimated A_V to about 0.03 mag at $z = 0.5$. A consistent opacity was reported by [Xie et al. \(2015\)](#) who studied the luminosity and redshifts of the quasar continuum of $\approx 90,000$ objects and estimated the intergalactic opacity at $z < 1.5$ as $\lambda_V \approx 0.02 h \text{ Gpc}^{-1}$.

Extinction by dust can also be measured from the hydrogen column densities of damped Lyman α absorbers (DLAs). Based on the Copernicus data, [Bohlin et al. \(1978\)](#) report a linear relationship between the total hydrogen column density, $N_{\text{H}} = 2N_{\text{H}_2} + N_{\text{HI}}$, and the color excess, $N_{\text{H}}/E(B - V) = 5.8 \times 10^{21} \text{ cm}^{-2} \text{ mag}^{-1}$, hence $N_{\text{H}}/A_V \approx 1.87 \times 10^{21} \text{ cm}^{-2} \text{ mag}^{-1}$ for $R_V = A_V/E(B - V) = 3.1$, which is a typical value for our Galaxy ([Cardelli et al. 1989](#); [Mathis 1990](#)). The result has been confirmed by [Rachford et al. \(2002\)](#) using FUSE data, who refined the slope between N_{H} and $E(B - V)$ to $5.6 \times 10^{21} \text{ cm}^{-2} \text{ mag}^{-1}$. Taking into account observations of the mean cross-section density of DLAs, $\langle n\sigma \rangle = (1.13 \pm 0.15) \times 10^{-5} h \text{ Mpc}^{-1}$ ([Zwaan et al. 2005](#)), the characteristic column density of DLAs, $N_{\text{HI}} \approx 10^{21} \text{ cm}^{-2}$, and the mean molecular hydrogen fraction in DLAs of about 0.4 – 0.6 ([Rachford et al. \(2002, their Table 8\)](#)), the intergalactic opacity λ_V at $z = 0$ is $\lambda_V \approx 1 - 2 \times 10^{-5} \text{ Mpc}^{-1}$, which is the result of [Xie et al. \(2015\)](#).

A low value of intergalactic opacity $\lambda_V \approx 0.02 \text{ Gpc}^{-1}$ indicates that the intergalactic space is almost transparent at $z = 0$. However, intergalactic opacity is redshift dependent. It increases with redshift and a transparent universe becomes significantly opaque at high redshifts. The opacity at high redshifts is caused by a high proper dust density due to the small volume of the Universe in the past. Since the dust density increases with redshift as $(1+z)^3$, the opacity increase is enormous and the total attenuation A_V can achieve a value

of 0.2 mag at $z = 1$ or even a value of 0.7 – 0.8 mag at $z = 3$ ([Vavryčuk 2018](#), his fig. 10a).

3 FITTING SUPERNOVAE MEASUREMENTS

The current supernovae compilations are comprised of about one thousand SNe Ia discovered and spectroscopically confirmed ([Sullivan et al. 2011](#); [Suzuki et al. 2012](#); [Campbell et al. 2013](#); [Betoule et al. 2014](#); [Rest et al. 2014](#); [Scolnic et al. 2018](#); [Riess et al. 2018](#)). Every SN Ia is described by its apparent rest-frame B-band magnitude, light curve shape, and colour correction. These parameters are used in the Tripp formula ([Tripp 1998](#); [Guy et al. 2007](#)) for determining the distance modulus $\mu(z)$ (Fig. 1),

$$\mu = m_B - M_B + \alpha x_1 - \beta c, \quad (1)$$

where m_B is the apparent rest-frame B-band magnitude, M_B is the absolute B-band magnitude, c and x_1 are the colour and stretch parameters, respectively, and the coefficients α and β are the global nuisance parameters to be calculated when seeking an optimum cosmological model. The distance modulus μ is related to the expansion history by the following equation,

$$\mu = 25 + 5 \log_{10}(d_L), \quad (2)$$

where d_L is the luminosity distance (in Mpc), which is expressed in flat ($\Omega_k = 0$) space as (e.g., [Subramani et al. 2019](#), their equation 12)

$$d_L = (1+z) \int_0^z \frac{cdz'}{H(z')}. \quad (3)$$

3.1 Λ CDM model

The standard Λ CDM cosmological model ([Planck Collaboration et al. 2016](#)) for the matter-dominated universe is described by the following equation

$$H^2(a) = H_0^2 \left[\Omega_m a^{-3} + \Omega_\Lambda + \Omega_k a^{-2} \right], \quad (4)$$

where

$$\Omega_m + \Omega_\Lambda + \Omega_k = 1. \quad (5)$$

The function $H(a)$ is the Hubble parameter characterizing the universe expansion with the scale factor $a = 1/(1+z)$, Ω_m is the total matter density contribution, Ω_k is related to the curvature of the Universe, and Ω_Λ is the dark energy contribution. Since measurements indicate that the Universe is nearly flat, Ω_k is zero in equation (4). Imposing the second time derivative of the scale factor a to be zero, $\ddot{a} = 0$, the transition from decelerating to accelerating expansion occurs at

$$a = \left(\frac{\Omega_m}{2\Omega_\Lambda} \right)^{1/3}, \quad (6)$$

which yields values $a = 0.69$ and $z = 0.67$ for the commonly used parameters $\Omega_m = 0.3$ and $\Omega_\Lambda = 0.7$.

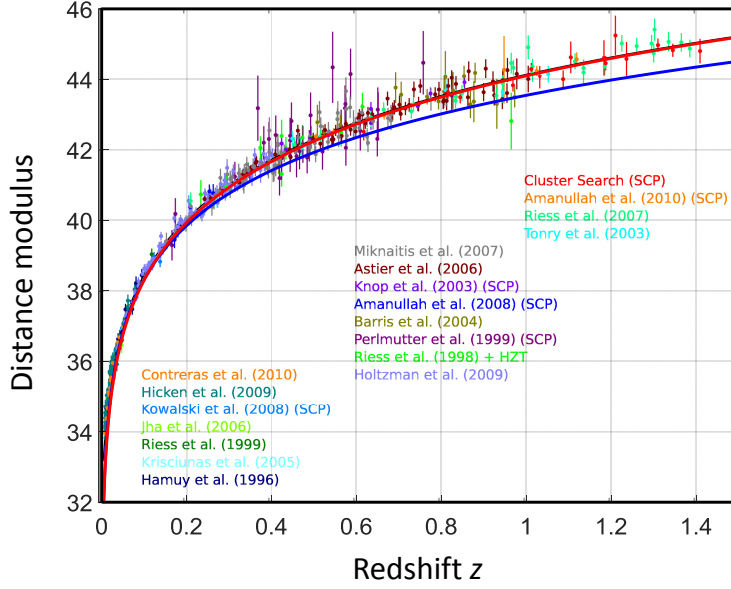


Figure 1. The Hubble diagram with SNe Ia measurements (Union2.1 dataset). Solid red line - the Λ CDM model with $\Omega_m = 0.3$, $\Omega_\Lambda = 0.7$, and $\Omega_k = 0$. Solid blue line - the cosmological model with $\Omega_m = 1.0$, $\Omega_\Lambda = 0$, and $\Omega_k = 0$. The data are not corrected for intergalactic opacity. Modified after Suzuki et al. (2012, their fig. 4).

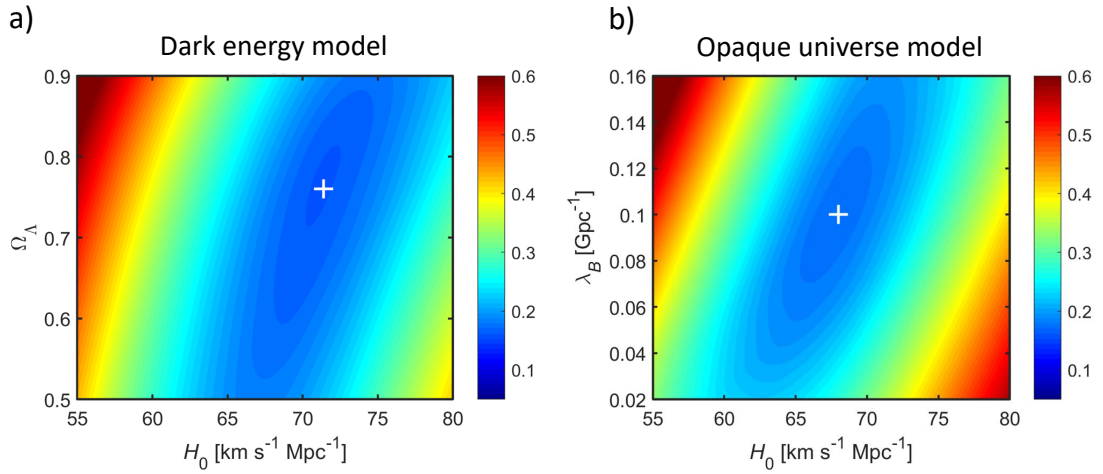


Figure 2. Inversion for optimum cosmological parameters of (a) the Λ CDM model and (b) the opaque universe model. The colour shows the mean of the absolute distance modulus residuals between the predicted model and the SNe Ia data as a function of: (a) the Hubble constant H_0 and the dark energy Ω_Λ , and (b) the Hubble constant H_0 and the B-band intergalactic opacity λ_B . Only the most accurate 552 SNe Ia with $z < 1.4$ and an error less than 0.50 mag are used. The optimum solutions marked by the white plus signs are defined by: (a) $H_0 = 71.4 \text{ km s}^{-1} \text{ Mpc}^{-1}$ and $\Omega_\Lambda = 0.77$ ($\alpha = 0.122$ and $\beta = 2.466$), and (b) $H_0 = 68.0 \text{ km s}^{-1} \text{ Mpc}^{-1}$ and $\lambda_B = 0.10 \text{ Gpc}^{-1}$ ($\alpha = 0.088$ and $\beta = 1.920$).

3.2 Opaque universe model

The universe opacity is quantified by the redshift-dependent optical depth, which is expressed in the B-band as follows (Vavryčuk 2017, his equation 19)

$$\tau_B = \int_0^z \lambda_B (1+z')^2 \frac{cdz'}{H(z')}. \quad (7)$$

where the Hubble parameter $H(z)$ is defined in equation (4) with $\Omega_m = 1.0$, $\Omega_\Lambda = 0$ and $\Omega_k = 0$. The parameter λ_B is the rest-frame B-band attenuation per unit ray path. Equa-

tion (7) takes into account an increase of the proper dust density with redshift as $(1+z)^3$ and a decrease of frequency-dependent opacity with z as $(1+z)^{-1}$ due to the $1/\lambda$ extinction law (Mathis 1990). Since wavelengths at the observer are longer due to redshift, they are less attenuated at the observer than at the source. In addition, a proper distance decreases with z as $(1+z)^{-1}$, but this is eliminated by an increase of light extinction with z as $(1+z)$ because the arrival rate of the photons suffers time dilation, often called the energy effect (Roos 2003).

Finally, the extinction correction of the distance modulus is expressed as

$$\Delta\mu = -2.5 \log_{10} e^{\tau_B(z)}. \quad (8)$$

3.3 Optimum model parameters

For fitting the two mentioned cosmological models, the Union2.1 SNe compilation (Suzuki et al. 2012) is used. The free parameters of the Λ CDM model (dark energy model) are the Hubble constant H_0 and the dark energy Ω_Λ . The free parameters of the opaque universe model are the Hubble constant H_0 and the B-band opacity λ_B ($\Omega_\Lambda = 0$). The optimum values of these parameters are found by a grid search. Only 552 most accurate SNe Ia with a distance modulus error less than 0.5 mag are considered. The mean distance modulus error is 0.2 mag. In order for the residua to have the same weight for different redshift intervals with a different number of the SNe Ia measurements, the mean absolute values of the residua are calculated in the following redshift bins: $z = [0, 0.025, 0.05, 0.1, 0.15, 0.20, 0.25, 0.30, 0.35, 0.40, 0.45, 0.5, 0.6, 0.8, 1.0, 1.2, 1.4]$. The width of bins is not uniform being narrower at low redshifts. In this way, the distribution of the SNe Ia in bins is more uniform having, respectively, the following numbers: [65, 75, 35, 27, 28, 27, 38, 33, 27, 28, 20, 37, 48, 37, 16, 11].

The misfit functions have a very shallow minimum for both considered models. For the opaque universe model, the best fit is found in the redshift interval $0 < z < 1.4$ for $H_0 = 68.0 \pm 2.5 \text{ km s}^{-1} \text{ Mpc}^{-1}$ and $\lambda_B = 0.10 \pm 0.03 \text{ Gpc}^{-1}$ (Fig. 2b). Analogously, the same data inverted for the optimum values of H_0 and Ω_Λ , describing the Λ CDM model, yield the best fit for $H_0 = 71.4 \pm 2.5 \text{ km s}^{-1} \text{ Mpc}^{-1}$ and $\Omega_\Lambda = 0.77 \pm 0.13$ (Fig. 2a). The uncertainty limits were calculated from the misfit function when all solutions with a fit at least of 99% of the best fit were accepted.

The residual Hubble plots are shown in Fig. 3. The optimum solutions have roughly comparable misfits for both models: 0.16 for the Λ CDM model (Fig. 3a), and 0.17 for the model of the opaque universe (Fig. 3b). However, as illustrated in Fig. 3c,d, the Λ CDM model performs slightly better than the opaque universe model, because of a better fit of the binned residua for redshifts less than 0.6. Nevertheless, the model of the opaque universe also accounts for the observed dimming of the SNe Ia within the confidence level of 95% (Fig. 3d).

Importantly, the optimum solutions are sensitive to the redshift interval of the SNe Ia used in the inversion. If the optimum model of the opaque universe is searched using the SNe Ia with redshifts $z \leq 0.6$ only, and the SNe Ia are grouped in the following redshift bins: $z = [0, 0.025, 0.05, 0.1, 0.15, 0.20, 0.25, 0.30, 0.35, 0.40, 0.45, 0.5, 0.6]$, we get $H_0 = 70.4 \pm 2.0 \text{ km s}^{-1} \text{ Mpc}^{-1}$ and $\lambda_B = 0.18 \pm 0.05 \text{ Gpc}^{-1}$ (Fig. 4). We see in Fig. 4b that the model fits the SNe measurements at $z < 0.6$ much better than in Fig. 3d, but a significant discrepancy appears at higher redshifts. A similar result was obtained by Goobar et al. (2002) and Riess et al. (2004), who concluded that the discrepancy at high redshifts excludes the SNe Ia dimming to be produced by intergalactic dust.

Note that the best estimate of H_0 for the Λ CDM model obtained by Riess et al. (2016) using the SNe Ia data is $73.24 \pm 1.74 \text{ km s}^{-1} \text{ Mpc}^{-1}$. The precision of the distance scale

was further improved by a factor of 2.5 by Riess et al. (2018). This value is within the uncertainty of the estimate of H_0 for the Λ CDM model obtained in this paper and shown in Fig. 2a. The accuracy of the presented value is, however, lower, because no specific analysis of M_B (which is degenerate with H_0) was performed and no further selection of the most accurate SNe Ia data was applied before the inversion. Interestingly, the Hubble constant H_0 in the Λ CDM model obtained from the Planck measurements of the cosmic microwave background is $H_0 = 67.4 \pm 0.5 \text{ km s}^{-1} \text{ Mpc}^{-1}$ (Planck Collaboration et al. 2018), being inconsistent with the results of Riess et al. (2018) and pointing to another difficulty of the Λ CDM model (Mörtsell & Dhawan 2018).

4 DISCUSSION AND CONCLUSIONS

The Λ CDM model explains satisfactorily current observations of the SNe Ia dimming by introducing dark energy into the Friedmann equations and considering the accelerating expansion of the Universe. Both concepts invoke, however, essential difficulties in physics. Dark energy causes negative pressure, which is required to explain the accelerating expansion. The pressure is extremely small, its magnitude being by 120 orders lower than a theoretical value predicted by quantum field theory (Koyama 2016, his equation 5). It is also unclear, why the dark energy has the same order of magnitude as the matter energy density just at the present epoch, although the matter density changed by a factor of 10^{42} during the evolution of the universe (Weinberg et al. 2013; Bull et al. 2016). Tension with the flat Λ CDM model arises also from a high-redshift Hubble diagram of supernovae, quasars, and gamma-ray bursts for redshifts $1.4 < z < 5$ (Lusso et al. 2019). In addition, the dark energy concept predicts the speeds of gravitational waves and light to be generally different (Sakstein & Jain 2017). However, observations of the binary neutron star merger GW170817 and its electromagnetic counterparts proved that both speeds coincide with a high accuracy ($< 5 \times 10^{-16}$). Hence, most of the dark energy models are disfavored (Ezquiaga & Zumalacárregui 2017). Other observational challenges to the Λ CDM model are summarized in Kroupa (2012), Kroupa (2015), Buchert et al. (2016) and Bullock & Boylan-Kolchin (2017).

By contrast, light extinction by intergalactic dust as a physically plausible origin of the SNe Ia dimming has been ignored or underrated. Its possible role in the SNe Ia dimming was discussed by several authors including Perlmutter et al. (1999) and Riess et al. (1998), but an opinion prevailed that the effect of intergalactic dust on the SNe Ia observations is minor. However, recent detailed studies of dust extinction in the SNe Ia spectra revealed that this issue is more complicated than so far assumed and that the standard extinction corrections applied uniformly to the SNe Ia observations were too simplified. For example, unexpected complexities were detected in reddening, being characterized by a variety of extinction laws with R_V going down to 1.4 (Amanullah et al. 2014, 2015; Gao et al. 2015). Consequently, approximate reddening-based corrections might bias the calculated distance modulus and lead to misinterpretations and to erroneously neglecting the role of intergalactic dust in the SNe Ia dimming (Ménard et al. 2010b).

This argument is supported by modelling performed in

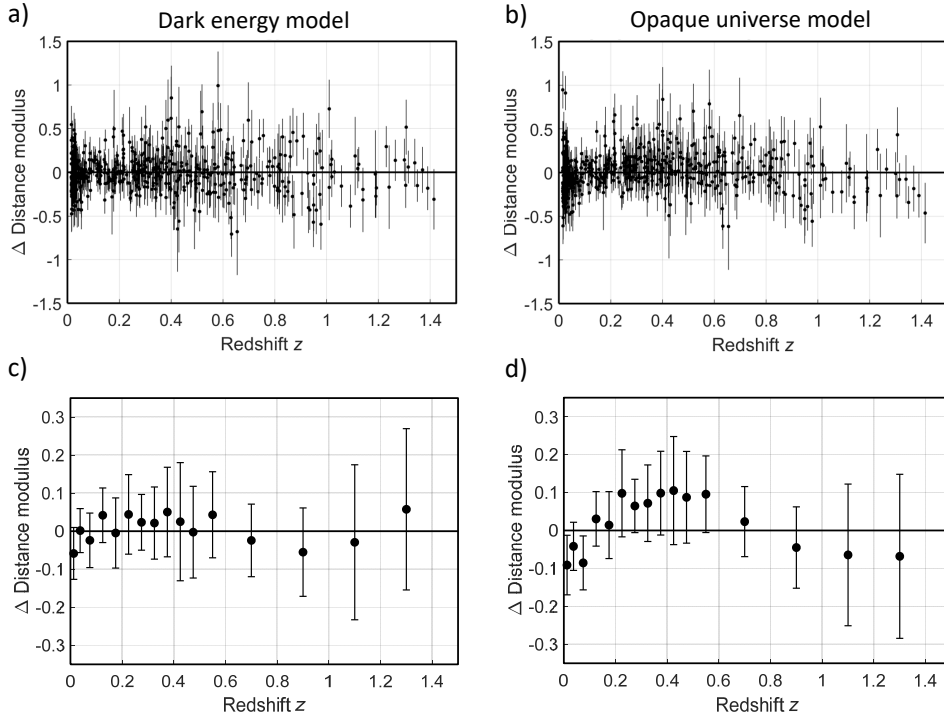


Figure 3. Residual Hubble plots for (a-b) the individual SNe Ia data and (c-d) the binned SNe Ia data. (a,c) The flat Λ CDM model with $H_0 = 71.4 \text{ km s}^{-1} \text{ Mpc}^{-1}$ and $\Omega_\Lambda = 0.77$. (b,d) The opaque universe model with $\lambda_B = 0.10 \text{ Gpc}^{-1}$ and $H_0 = 68.0 \text{ km s}^{-1} \text{ Mpc}^{-1}$. The error bars in (c-d) show the 95% confidence intervals. Data are taken from Suzuki et al. (2012).

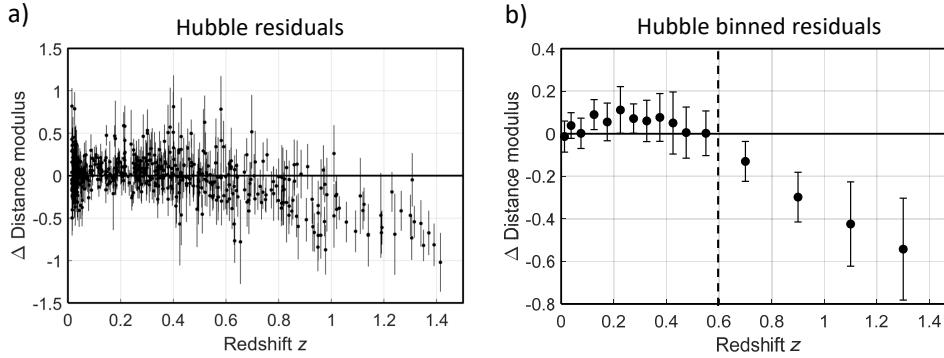


Figure 4. Residual Hubble plots for (a) the individual and (b) binned SNe Ia data for the opaque universe model with $\lambda_B = 0.18 \text{ Gpc}^{-1}$ and $H_0 = 70.4 \text{ km s}^{-1} \text{ Mpc}^{-1}$. The vertical dashed line in (b) denotes the upper redshift limit of the SNe Ia data considered in the inversion. The error bars in (b) show the 95% confidence intervals. Data are taken from Suzuki et al. (2012).

this paper, which shows that the opaque universe model can fit the observations almost equally well as the Λ CDM model, if inverted in the whole redshift interval of the SNe Ia observations. The found optimum B-band intergalactic opacity is $\lambda_B = 0.10 \pm 0.03 \text{ Gpc}^{-1}$ and the Hubble constant is $H_0 = 68.0 \pm 2.5 \text{ km s}^{-1} \text{ Mpc}^{-1}$. Since the redshift-distance relation differs in the Λ CDM model and in the opaque universe model by a factor of about 1.5–2, the value $\lambda_V \approx 0.02 h \text{ Gpc}^{-1}$ of Xie et al. (2015) recalculated to the opaque universe model is $\lambda_V \approx 0.04 \text{ Gpc}^{-1}$. Taking into account that λ_B is

expressed as $\lambda_B = \lambda_V(R_V + 1)/R_V$, we get $\lambda_B \approx 0.05 \text{ Gpc}^{-1}$ for $R_V = 3.1$ (Cardelli et al. 1989). Hence, the retrieved value of $\lambda_B \approx 0.10 \pm 0.03 \text{ Gpc}^{-1}$ is higher than that expected from independent observations but still within reasonable limits.

The presented results emphasize that the issue of the accelerating expansion of the Universe is not yet definitely resolved and it should be revisited in a more thorough way in future. Obviously, the opaque universe model as an alternative to the Λ CDM model is attractive, because it avoids puzzles and controversies associated with dark energy and

the accelerating expansion. The opaque universe model can straightforwardly explain anisotropic Hubble residuals by assuming a slightly anisotropic distribution of intergalactic dust instead of interpreting them by anisotropic expansion of the Universe (Schwarz & Weinhorst 2007; Wang & Wang 2014; Javanmardi et al. 2015). The model also successfully explains phenomena related to the extragalactic background light, such as its bolometric intensity and the luminosity density evolution with redshift (Vavryčuk 2017), and properties of the cosmic microwave background (Vavryčuk 2018).

ACKNOWLEDGEMENTS

I thank an anonymous reviewer for his detailed and helpful comments and Nao Suzuki for permitting to reproduce fig. 4 from Suzuki et al. (2012).

REFERENCES

- Aguirre A. N., 1999a, *ApJ*, **512**, L19
Aguirre A., 1999b, *ApJ*, **525**, 583
Aguirre A., Haiman Z., 2000, *ApJ*, **532**, 28
Amanullah R., et al., 2014, *ApJ*, **788**, L21
Amanullah R., et al., 2015, *MNRAS*, **453**, 3300
Betoule M., et al., 2014, *A&A*, **568**, A22
Blome H. J., Priester W., 1985, *Ap&SS*, **117**, 327
Bohlin R. C., Savage B. D., Drake J. F., 1978, *ApJ*, **224**, 132
Buchert T., Coley A. A., Kleinert H., Roukema B. F., Wiltshire D. L., 2016, *International Journal of Modern Physics D*, **25**, 1630007
Bull P., et al., 2016, *Physics of the Dark Universe*, **12**, 56
Bullock J. S., Boylan-Kolchin M., 2017, *Annual Review of Astronomy and Astrophysics*, **55**, 343
Campbell H., et al., 2013, *ApJ*, **763**, 88
Cardelli J. A., Clayton G. C., Mathis J. S., 1989, *ApJ*, **345**, 245
Carroll S. M., Press W. H., Turner E. L., 1992, *ARA&A*, **30**, 499
Chelouche D., Koester B. P., Bowen D. V., 2007, *ApJ*, **671**, L97
Einstein A., 1917, *Sitzungsberichte der Königlich Preußischen Akademie der Wissenschaften (Berlin)*, pp 142–152
Ezquiaga J. M., Zumalacárregui M., 2017, *Phys. Rev. Lett.*, **119**, 251304
Gao J., Jiang B. W., Li A., Li J., Wang X., 2015, *ApJ*, **807**, L26
Goobar A., Bergström L., Mörtzell E., 2002, *A&A*, **384**, 1
Guy J., et al., 2007, *A&A*, **466**, 11
Javanmardi B., Porciani C., Kroupa P., Pflamm-Altenburg J., 2015, *ApJ*, **810**, 47
Jones D. O., et al., 2018, *ApJ*, **857**, 51
Koyama K., 2016, *Reports on Progress in Physics*, **79**, 046902
Kroupa P., 2012, *Publications of the Astronomical Society of Australia*, **29**, 395
Kroupa P., 2015, *Canadian Journal of Physics*, **93**, 169
Lusso E., Piedipalumbo E., Risaliti G., Paolillo M., Bisogni S., Nardini E., Amati L., 2019, arXiv e-prints, p. arXiv:1907.07692
Mathis J. S., 1990, *ARA&A*, **28**, 37
Ménard B., Scranton R., Fukugita M., Richards G., 2010a, *MNRAS*, **405**, 1025
Ménard B., Kilbinger M., Scranton R., 2010b, *MNRAS*, **406**, 1815
Mörtzell E., Dhawan S., 2018, *J. Cosmology Astropart. Phys.*, **2018**, 025
Muller S., Wu S.-Y., Hsieh B.-C., González R. A., Loinard L., Yee H. K. C., Gladders M. D., 2008, *ApJ*, **680**, 975
Nugent P., Kim A., Perlmutter S., 2002, *Publications of the Astronomical Society of the Pacific*, **114**, 803
Peebles P. J., Ratra B., 2003, *Reviews of Modern Physics*, **75**, 559
Perlmutter S., et al., 1999, *ApJ*, **517**, 565
Planck Collaboration et al., 2016, *A&A*, **594**, A13
Planck Collaboration et al., 2018, arXiv e-prints, p. arXiv:1807.06209
Rachford B. L., et al., 2002, *ApJ*, **577**, 221
Rest A., et al., 2014, *ApJ*, **795**, 44
Riess A. G., 2000, *PASP*, **112**, 1284
Riess A. G., et al., 1998, *AJ*, **116**, 1009
Riess A. G., et al., 2004, *ApJ*, **607**, 665
Riess A. G., et al., 2016, *ApJ*, **826**, 56
Riess A. G., et al., 2018, *ApJ*, **861**, 126
Roos M., 2003, *Introduction to Cosmology*, Third Edition
Sahni V., Starobinsky A., 2000, *International Journal of Modern Physics D*, **9**, 373
Sakstein J., Jain B., 2017, *Phys. Rev. Lett.*, **119**, 251303
Schwarz D. J., Weinhorst B., 2007, *A&A*, **474**, 717
Scolnic D. M., et al., 2018, *ApJ*, **859**, 101
Subramani V. B., Kroupa P., Shenavar H., Muralidhara V., 2019, *MNRAS*, p. 1960
Sullivan M., et al., 2011, *ApJ*, **737**, 102
Suzuki N., et al., 2012, *ApJ*, **746**, 85
Tripp R., 1998, *A&A*, **331**, 815
Vavryčuk V., 2017, *MNRAS*, **465**, 1532
Vavryčuk V., 2018, *MNRAS*, **478**, 283
Wang J. S., Wang F. Y., 2014, *MNRAS*, **443**, 1680
Weinberg S., 1989, *Reviews of Modern Physics*, **61**, 1
Weinberg D. H., Mortonson M. J., Eisenstein D. J., Hirata C., Riess A. G., Rozo E., 2013, *Phys. Rep.*, **530**, 87
Xie X., Shen S., Shao Z., Yin J., 2015, *ApJ*, **802**, L16
Zwaan M. A., van der Hulst J. M., Briggs F. H., Verheijen M. A. W., Ryan-Weber E. V., 2005, *MNRAS*, **364**, 1467